Earth Surf. Dynam., 7, 345–360, 2019
https://doi.org/10.5194/esurf-7-345-2019

Earth Surface Dynamics
Open Access
EGU

Rainfall intensity bursts and the erosion of soils: an analysis highlighting the need for high temporal resolution rainfall data for research under current and future climates

David L. Dunkerley

School of Earth Atmosphere and Environment, Faculty of Science, Monash University, Victoria 3800, Australia

Correspondence: David L. Dunkerley (david.dunkerley@monash.edu)

Received: 16 December 2018 – Discussion started: 7 January 2019
Revised: 11 March 2019 – Accepted: 25 March 2019 – Published: 15 April 2019

Abstract. Many land surface processes, including splash dislodgment and downslope transport of soil materials, are influenced strongly by short-lived peaks in rainfall intensity but are less well accounted for by longer-term average rates. Specifically, rainfall intensities reached over periods of 10–30 min appear to have more explanatory power than hourly or longer-period data. However, most analyses of rainfall, and particularly scenarios of possible future rainfall extremes under climate change, rely on hourly data. Using two Australian pluviograph records with 1 s resolution, one from an arid and one from a wet tropical climate, the nature of short-lived "intensity bursts" is analysed from the raw inter-tip times of the tipping bucket gauges. Hourly apparent rainfall intensities average just 1.43 mm h^{-1} at the wet tropical site and 2.12 mm h^{-1} at the arid site. At the wet tropical site, intensity bursts of extreme intensity occur frequently, those exceeding 30 mm h^{-1} occurring on average at intervals of < 1 d and those of > 60 mm h^{-1} occurring on average at intervals of < 2 d. These bursts include falls of 13.2 mm in 4.4 min, the equivalent of 180 mm h^{-1}, and 29 mm in 12.6 min, equivalent to 138 mm h^{-1}. Intensity bursts at the arid site are much less frequent, those of 50–60 mm h^{-1} occurring at intervals of ~ 1 month; moreover, the bursts have a much shorter duration. The aggregation of rainfall data to hourly level conceals the occurrence of many of these short-intensity bursts, which are potentially highly erosive. A short review examines some of the mechanisms through which intensity bursts affect infiltration, overland flow, and soil dislodgment. It is proposed that more attention to resolving these short-lived but important aspects of rainfall climatology is warranted, especially in light of possible changes in rainfall extremes under climate change.

1 Introduction

Soil erosion is an important risk factor for future pastoral and agricultural production, as well as water quality, and is considered highly likely to be affected by climate change (Nearing et al., 2004; Klik and Eitzinger, 2010; Mullan et al., 2012; Segura et al., 2014; Garbrecht et al., 2015; Mondal et al., 2015; Sharratt et al., 2015; Li and Fang, 2016; Giang et al., 2017). Soil erosion consequently bears on global food security, in addition to the more direct effects of changing climate on crop yields (Rhodes, 2014), and a need for adaptations to protect agricultural productivity has been highlighted (Blanco and Lal, 2008). The erosion of soils by rainsplash and flowing water involves a multitude of processes acting across spatial and temporal scales, from momentary splash dislodgment of a small particle to sediment remobilisation from temporary storage in locations such as alluvial fans, foot slopes, or floodplains. There are many reasons for seeking to understand and track soil erosion in the contemporary landscape and for working towards an understanding of

how it may respond to climate change. The burgeoning human population and increased need for food, fuel, and fibre is placing increasing demands on cultivated and rangeland soils, for which some contemporary erosion rates are already considered unsustainable (Panagos et al., 2015). Simultaneous changes in global and regional hydroclimates, related to global warming and shifts in the nature of the hydrologic cycle, may result in increased frequency and erosivity of rainfall events (Hatfield et al., 2013), as well as related ecosystem changes including in floristics, plant architecture, and soil moisture content. At the same time, growth in urban areas and populations, and the associated impervious urban land surfaces, appears to be resulting in increased risk of urban flash flooding and associated sediment transport, especially in peri-urban areas (Esposito et al., 2018), though this may be partially offset by the growing adoption of "sponge city" and similar approaches to building more absorbent cities (Li et al., 2017, 2018; Dong et al., 2018). Archer and Fowler (2018) have illustrated the effects of short-term "intensity bursts" in UK flooding, emphasising that short-period intensity was more significant than total rainfall. Additionally, there are indications that fire regimes, especially the occurrence of large wildfires, will be altered by climate change (van Bellen et al., 2010; Bowman et al., 2013; Harvey, 2016). As will be discussed below, post-fire landscapes are especially vulnerable to intense soil erosion. In addition to these considerations and others that could be listed, soils themselves may alter in response to climate change, with changes in organic matter content and the activity of soil biota possibly modifying soil structure, aggregation, and erodibility (Karmakar et al., 2016). It is clear, therefore, that multiple factors may result in different rates or mechanisms of soil erosion in coming decades, posing a significant challenge for the informed management of agricultural and other soils.

Extreme rainfalls, especially at short timescales of minutes or tens of minutes, are widely recognised as important drivers of soil erosion. Some of the field evidence will be summarised later. Despite this, they have received less attention than more lumped measures of rainfall, such as daily totals, from which change detection is undertaken by such methods as tallying the number of daily rainfalls exceeding the historic 95th percentile (or some other statistic) of daily rainfalls (Schär et al., 2016; Dunkerley, 2018). For example, in comparing 20th century data with model scenarios for 2081–2100, O'Gorman and Schneider (2009) employed the 99.9th percentile daily rainfall as a measure of extreme rainfall. They report that in the tropics, 20th century extreme daily rainfalls exceeded 50 mm, but in model scenarios for the late 21st century this increased to about 70 mm (O'Gorman and Schneider, 2009, Fig. 1). Whilst extreme daily totals such as these are an informative measure for the purposes of climate science, in the context of soil erosion, they do not provide sufficient resolution to understand erosional events. Soil loss is often most successfully accounted for by measures of sub-daily rainfall intensity over minutes or tens of minutes (see below). Attempts to explore sub-daily extreme rainfalls are hampered because many available rainfall data sets, as well as scenarios of future rainfalls under climate change, commonly provide only daily or hourly resolution (Guerreiro et al., 2018). In analysing sub-daily rainfall data from 5347 stations globally, Monjo (2016) reported that only 17.8 % had a reporting frequency of 1 h, and about 75 % reported rainfalls 2–4 times per day, 42.2 % having a 6 h resolution. Some workers have focussed on common, rather than extreme, rainfalls. Pendergrass and Deser (2017) for instance argued that ordinary rainfalls deliver most rain and release most latent heat and are thus more relevant to climate studies. Studies of rainfall extremes employing daily rainfall amounts include Donat et al. (2013) and Keggenhoff et al. (2014); studies of extremes relying on hourly totals include Sun et al. (2017), who analysed rainfall extremes over eastern China, Cortés-Hernández et al. (2016) for eastern Australia and Beranova et al. (2018) for the Czech Republic. Similarly, many studies of the secular trends in extreme events rely on hourly or daily rainfall depth data (Costa and Soares, 2008; Peralta-Hernandez et al., 2009; Formayer and Fritz, 2017; de Waal et al., 2017; Lupikasza et al., 2017, Yu et al., 2017). Yet other studies rely on data aggregated to longer periods, such as the 2–3 h aggregation used by Luo and Wang (2013). There are exceptions to the general reliance on daily and hourly rainfall data, which include Yilmaz and Perera (2015), who examined 10 and 30 min data, as well as hourly and longer aggregations, in a study of extreme rainfalls in Victoria, Australia. Many studies of rainfall occurrence, including extremes, consequently use parameters selected under constraints of data availability. These may involve average intensities tallied using data pooled from many rain days and which conceal variation among days. For instance, Polemio and Lonigro (2015) used a "monthly rainfall intensity", which is the monthly rainfall depth scaled by the number of rain days in that month. Others use a similar "daily rain intensity" (e.g. Nandargi and Mulye, 2012) or the "simple daily intensity index", which is defined as the ratio of the annual total precipitation to the number of wet days (Hatzaki et al., 2010; Zhang et al., 2011; Gao et al., 2018). Many such indices, with their very limited temporal resolution, are likely to offer restricted explanatory power in relation to splash and water erosion of soils or to other land surface hydrological processes.

Motivated by the foregoing, the goal of the present paper is to present a brief overview of short-term rainfall extremes, focussing primarily on what are here referred to as intensity bursts: short periods of intense rainfall contained within longer events of lower overall intensity. This terminology echoes that of Peters and Christensen (2002), who explored the burst-like behaviour of rainfall, which they likened to the sporadic temporal occurrence of earthquakes or mass movements. To support the objective of highlighting the nature and importance of these short-duration bursts, a brief review is provided of some of the mechanisms through which

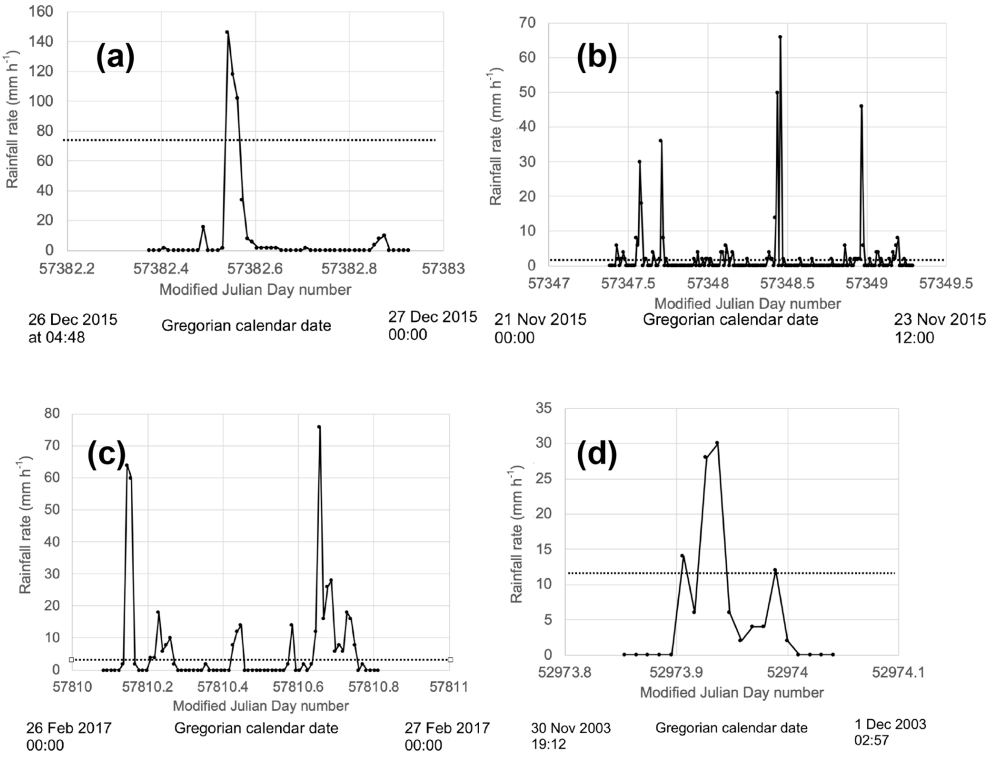

Figure 1. Examples of intensity bursts in rainfall records from the field sites, shown using data aggregated to 15 min totals. Each dot represents a 15 min period. Field locations: **(a–c)** MM and **(d)** FG. The four intensity plots shown here each show the entirety of a rainfall event defined using MIT = 6 h (refer to text for details). Each event begins with the first rainfall and ends with the last rainfall; preceding and subsequent observations showing zero rainfall rate are not included in the events. Event **(a)** is mostly rainless but includes a single very intense burst; events **(b)** and **(c)** contain one or more bursts together with periods of lower intensity; event **(d)** shows continuous rainfall with a central intensity burst. In each case the dotted lines indicate the average intensity of the rainfall event.

intensity bursts drive processes such as surface ponding and the splash dislodgment of soil particles. However, as a first step, using rainfall data from the Australian desert and wet tropics, intensity bursts are explored quantitatively using tipping bucket rain gauge data with a 1 s temporal resolution. Intensity is assessed from the time between successive tipping bucket tip events, with no aggregation. It is the aim of this short overview to highlight the need for more study of rainfall behaviour at high temporal resolution, especially to characterise intensity bursts in a way that will facilitate further exploration of their influence on surface processes. There is currently little or no literature exploring the likely changes in short-lived intensity bursts under future climate change. In a sense this is unsurprising, as there has been little investigation of intensity bursts, even in empirical data collected under the present climate. Nevertheless, it will be argued here that short-term intensity bursts warrant further consideration, especially in relation to surface hydrology and soil erosion.

What is meant by an intensity burst?

It is appropriate to begin by further describing intensity bursts. The analysis presented below seeks both to illustrate the nature of these bursts at two field locations and to highlight the important differences between the kinds of indices commonly adopted in climate science and those employed in research on soil erosion and related land surface processes. The expression intensity burst is used here without a rigorous, formal definition, to refer to periods of very intense rain that occupy a small fraction of the duration of a longer enclosing event in which the typical intensity is lower. Examples from the two Australian field locations used in the remainder of this paper are shown in Fig. 1. The literature provides no established definitions with which to define an intensity burst. Here, the use of a threshold intensity of 20 mm h^{-1} is adopted. This is the intensity above which rainfall intensity is classified as "extreme" by Tokay and Short (1996). The contrast between the mean intensity of rainfall events and the intensity of bursts that occur within them can be marked. The intensity of the bursts shown in Fig. 1 and the mean intensity of the rainfall events within which they occurred are set out in Table 1.

Table 1. Details of rainfall events defined using MIT = 6 h, together with the mean rainfall intensity of the event and the peak burst intensities evident in data aggregated to 15 min rainfall totals. See text for details.

Location	Start date of rainfall event (MJD)	End date of rainfall event (MJD)	Duration of event (h)	Depth of event (mm)	Mean rainfall intensity of event ($mm\,h^{-1}$)	Peak intensities of burst(s) within event from 15 min data ($mm\,h^{-1}$)
MM	57 382.40	57 349.24	13.9	42.8	1.32	146
MM	57 347.42	57 349.24	43.6	46.8	0.98	30, 36, 67, 48
MM	57 810.12	57 810.77	15.4	45.8	2.97	64, 76
FG	52 973.90	52 973.99	2.3	27.0	11.63	30

2 Field sites and methods of data collection and processing

2.1 Field locations and the tipping-bucket pluviograph data

Data from two contrasting field locations are analysed here – one arid and one wet tropical. The wet tropical field location was near the township of Millaa Millaa, on the Atherton Tablelands, within the wet tropics of far northern Queensland, Australia. The site (hereafter designated MM) was located at 650 m a.s.l. and 40 km inland from the Coral Sea coastline. Local mean annual rainfall is 2290 mm (2001–2018 data; http://www.bom.gov.au/, last access: 20 March 2019), primarily falling in a wet season from January to May. The rain is orographically enhanced in moist SE trade winds that rise over rugged uplands immediately inland of the coast. The data analysed here were recorded during 2014–2017 and yielded a total of 9.15 m of rainfall (and > 45 000 tipping bucket events). The dryland site was located on the Fowlers Gap Arid Zone Research Station (hereafter FG), located about 100 km north of the regional city of Broken Hill, in the arid far west of New South Wales, Australia. Annual rainfall averages 236 mm (2004–2018 data; http://www.bom.gov.au/) but varies markedly from year to year, related to the El Niño–Southern Oscillation (ENSO) cycle of drought and wet years. Some aspects of the rainfall climatology of this site, including the nature of rainfall in wet and dry years and the intensity variations at intra-event timescales, have been described previously (Dunkerley, 2010, 2013). Fowlers Gap is located ∼ 950 km from the Australian east coast and more than 450 km from the nearest coastline in Spencer Gulf, South Australia. The continuous record from this site was collected in the period 2002–2012 and records about 2.6 m of rainfall (∼ 5300 bucket tip events).

The raw data analysed here consist of 0.2 mm tipping bucket events (MM) and 0.5 mm events (FG), logged with a 1 s resolution and analysed without any time aggregation. There were no missing data from either rainfall record. The data logger files of bucket tip events that were recorded in the Gregorian calendar were converted to Modified Julian Days (MJD), using double-precision FORTRAN routines from the International Astronomical Union's "SOFA" (Standards of Fundamental Astronomy) subroutine library (http://www.iausofa.org/, last access:). Using the SOFA subroutine "CAL2JD", hourly and daily rainfalls were extracted, as well as counts of rain days and rainless days. Rainfall events were identified using the minimum inter-event time (MIT) approach (Dunkerley, 2008). This identifies separate rainfall events by requiring a rainless period of a nominated duration before each event. In the present work, this was taken to be 6 h with no rainfall. The choice of value for the MIT affects the delineation of rainfall events considerably (Dunkerley, 2008) but does not affect the identification of intensity bursts, since this is done from the unaggregated data on inter-tip times.

2.2 Brief descriptions of the rainfall characteristics at the MM and FG field sites

At MM, the discrete rainfall events defined by the 6 h MIT (N, the number of identified rainfall events, was 652) lasted on average 18.6 h and delivered 21.3 mm at an average intensity of $2.2\,mm\,h^{-1}$. The average rain day (day with at least one bucket tip, i.e. ≥ 0.2 mm) amount was 11.7 mm, yielding an average daily mean intensity of $0.48\,mm\,h^{-1}$. From a corresponding analysis of rain hours (there were 6409 h with ≥ 0.2 mm rainfall), the average hourly rainfall was 1.43 mm (average hourly intensity $1.43\,mm\,h^{-1}$). The 95th, 99th, and 99.9th percentiles of hourly rainfall intensity were 5, 13, and $32.1\,mm\,h^{-1}$. The maximum hourly rainfall was 60.6 mm. At a daily scale, the rain was intermittent, and on average, 66 % of the hours on a rain day were rainless, and this accounts for the difference between daily and hourly mean rainfalls. These figures suggest that the rainfall climatology of the MM study site is characterised by quite low intensities, falling in events that typically last less than a day. However, aggregating the data to daily or hourly level involves sacrificing the resolution of the raw bucket tip data; the data on intensity bursts, examined shortly, present quite a different description of the rainfall.

At FG, the average rain day (day with at least one bucket tip, i.e. ≥ 0.5 mm) amount was 7.58 mm, yielding an average

daily mean intensity of 0.32 mm h^{-1}. For rain hours (N = 1259 h), the mean amount was 2.12 mm (average hourly intensity 2.12 mm h^{-1}). The 95th, 99th, and 99.9th percentiles of hourly rainfall intensity were 8, 14.5, and 26.1 mm h^{-1}. The maximum hourly rainfall was 23.5 mm. In total, 85.1 % of hours in the record were rainless. The fact that the hourly rainfall at FG was 6.6 times larger than the daily intensity reflects the high intermittency of rain during a rain day. At MM, the hourly rainfall was only 2.9 times larger than the daily intensity, reflecting lower intermittency of rain on rain days at the wet tropical site.

In summary, average wet day rainfalls and average daily intensities were both larger at MM. However, average wet hour rainfalls were larger at FG. This reflects the shorter duration and lesser intermittency of rain in the arid conditions at FG. Thus, the level of aggregation of the rainfall data – daily or hourly – affects the apparent intensity of the rainfall. This effect is of considerable potential importance when seeking to understand soil erosion and land surface hydrology. Moreover, actual intensities during rainfall, assessed over sub-daily durations that involve less loss of resolution, reveal quite different intensities than those just reviewed, as will be shown next.

In what follows, the intensity was calculated with minimal loss of resolution from the raw, unaggregated inter-tip times (ITTs) between bucket tips (the time taken for 0.2 or 0.5 mm of rain to be recorded). During long ITTs, reflecting low-intensity rainfall, there may be fluctuations in intensity or periods of complete cessations of rainfall as the bucket progressively fills. In contrast, during the short ITTs associated with extreme intensity bursts, it is possible to be confident that the intensity calculated from the ITT is indicative of the rainfall intensity as the bucket filled through seconds or minutes. Intensities were extracted from the data logger files for ITTs in the range 5–0.1 min. Owing to difference in the tipping bucket sizes, the ITT indicative of at least 30 mm h^{-1} at FG is 1 min, and at MM, 0.4 min. The sequences of time-varying ITTs provide an indication of the intensity of rain from moment to moment. However, the character of intensity bursts was assessed by examining the lengths of uninterrupted sequences of short ITTs whose duration did not exceed a chosen threshold value, such as 30 s. Such runs of short ITTs represent sustained intensities exceeding a threshold intensity determined by the nominated ITT. For purposes of reporting, these sequences are here termed "runs" of short ITTs. The durations of all runs for ITTs of up to 5 min were extracted from the data for MM and FG. It is straightforward to determine the minimum intensity required to result in runs of short ITTs of specified duration for the two field sites. Thus, at MM, runs of tips occurring at least every 60 s represent rainfall of at least 12 mm h^{-1} ("very heavy" rainfall, according to the classification of Tokay and Short, 1996). Runs of tips occurring at least every 30 s would represent rainfall of at least 24 mm h^{-1}, and tips occurring at least every 15 s correspond to intensities of at least 48 mm h^{-1}.

The lengths of runs of short ITTs were extracted from the unaggregated bucket tip records. From these data, the relationships among the duration, depth, and intensity of the intensity bursts were analysed. The start and end dates of each burst were recorded from the MJD data, and from these data the frequency of occurrence of bursts at the two field sites and the length of the time between the occurrence of successive bursts were recorded.

3 Results

At wet tropical Millaa Millaa (MM), of the 45 737 ITTs, 94.4 % were shorter than 60 min, 70.0 % were shorter than 5 min, and 36.5 % shorter than 1 min (Fig. 2). The median ITT was 1.8 min, corresponding to an intensity of 6.7 mm h^{-1}. At arid Fowlers Gap (FG), of the 5353 ITTs, 88.0 % were shorter than 60 min and 49 % shorter than 5 min, and the median value was 5.2 min, corresponding to an intensity of 5.7 mm h^{-1}. The median ITTs thus indicate intensities that are 4.7 times larger (MM) and 2.7 times larger (FG) than the average rain hour intensity reported above, which was in turn 2.9–6.6 times larger than the daily intensities. Unsurprisingly, the extent of temporal aggregation results in wide variations in the apparent intensity of the rainfall. This is illustrated in Fig. 3, which compares the rainfall rates determined from the unaggregated ITTs with the same data but aggregated to 15 min and 1 h totals, from a single MM rainfall event defined using MIT = 6 h. The event lasted 43.6 h and delivered 46.8 mm of rain at an average intensity of 0.98 mm h^{-1}. The raw ITT data show intensity bursts of up to 240 mm h^{-1}, whereas the 15 min data show bursts of only about 67 mm h^{-1} or less than one-third as intense; the 1 h data show the largest burst at only 13 mm h^{-1}. Moreover, the first two intensity peaks show the effect of burst duration, the first peak being more intense in the raw ITT data and the 1 h data, but the second (shorter) burst is more intense in the 15 min data.

In terms of the development of surface ponding, overland flow, and the splash dislodgment of soil, runs of short ITTs represent periods of sustained high intensity – an intensity burst. Details of runs of short ITTs corresponding to intensities of at least 20 mm h^{-1} (extreme intensity) at both field sites are presented in Table 2.

Some remarkable runs of short ITTs at MM included 270 successive bucket tips less than 30 s apart. The intensity burst lasted for 49.4 min, delivering 54 mm, the equivalent of a mean intensity of 65.6 mm h^{-1}. The longest run of ITTs shorter than 15 s lasted for 12.6 min, delivering 29 mm in 145 successive tips, the equivalent of 138 mm h^{-1}. The longest run of tips occurring at least every 6 s, representing an intensity of at least 120 mm h^{-1}, consisted of 66 successive tip events, delivering 13.2 mm in 4.4 min, the equivalent of 180 mm h^{-1}. Clearly, within these bursts, there must occur sub-periods during which the intensity is higher and the ITT

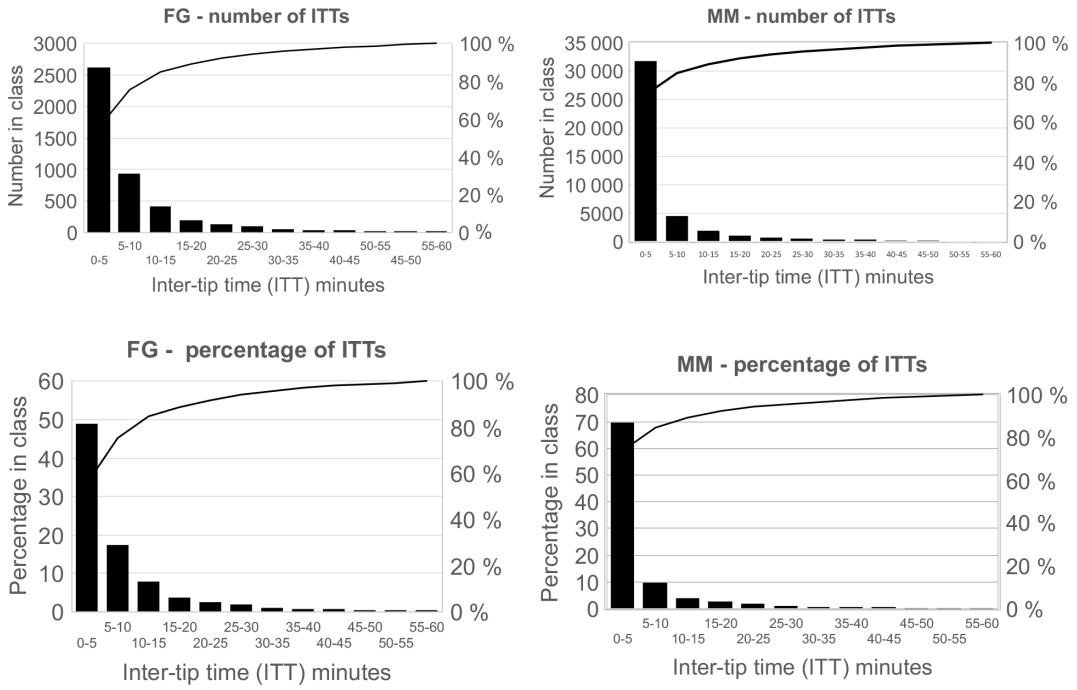

Figure 2. Distributions of the number of inter-tip times (ITTs) in the rainfall records from the Fowlers Gap (FG) and Millaa Millaa (MM) field sites, in 5 min bins, for all ITTs up to 1 h. Also shown is the percentage of ITTs falling into each ITT class.

Table 2. Details of runs of short ITTs forming intensity bursts at the two field sites. The ITT values listed in column 1 were selected to represent intensities of approximately 30, 40, 50, 60, and 120 mm h^{-1}. The ITT durations, and the numbers of ITTs shown in column 4, differ between the sites owing to the 0.2 mm sensitivity of the tipping bucket gauge at MM and the 0.5 mm sensitivity at FG. Note also that the average time between the commencement of runs of short ITTs in column 8 is expressed in hours for MM but in days for FG.

Millaa Millaa (MM)							
ITT (min)	*N*	Average number of ITTs per run	Max number of ITTs per run	Average duration of run (min)	Max duration of run (min)	Average intensity of runs (mm h^{-1})	Average time between commencement of runs (hour)
0.4	1854	4.5	149	1.08	22.5	44.9	15.6
0.3	1400	4.4	146	0.88	17.2	54.4	20.6
0.25	1112	4.3	145	0.77	12.6	62.7	26.1
0.2	695	3.8	143	0.54	11.7	80.5	39.1
0.1	286	1.45	66	0.097	4.4	196.0	92.3
Fowlers Gap (FG)							
ITT (min)	*N*	Average number of ITTs per run	Max number of ITTs per run	Average duration of run (min)	Max duration of run (min)	Average intensity of runs (mm h^{-1})	Average time between commencement of runs (day)
1.0	217	5	58	2.71	21.3	45.2	15.8
0.8	184	5	50	2.15	15.9	52.1	18.7
0.6	133	4	49	1.57	15.3	65.8	25.4
0.5	92	4	48	1.45	14.7	75.9	36.9
0.25	27	2	9	0.50	1.95	134.4	133.1

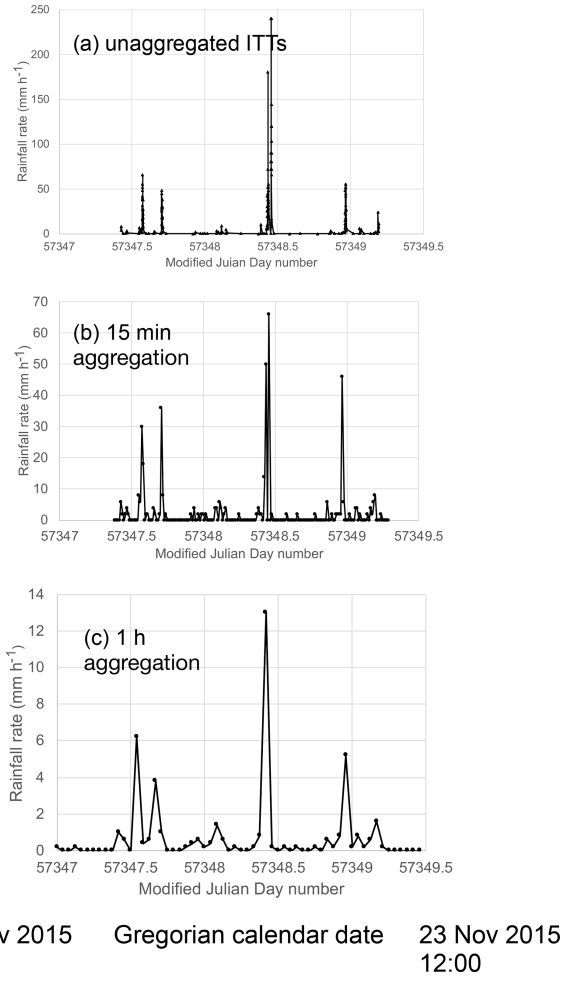

Figure 3. Effect of time aggregation on the appearance of intensity bursts in the MM data, for a rainfall event starting at Modified Julian Day 57 347.42 (on 21 November 2015) and ending at 57 349.24 (on 23 November 2015). **(a)** Unaggregated ITTs. **(b)** Data aggregated to 15 min rainfall totals. **(c)** Data aggregated to 1 h totals. Note that the scale of rainfall intensities differs among the three graphs, owing to the more intense bursts evident in the less aggregated data. Gregorian dates for the endpoints of the date axis are shown at the bottom of the figure.

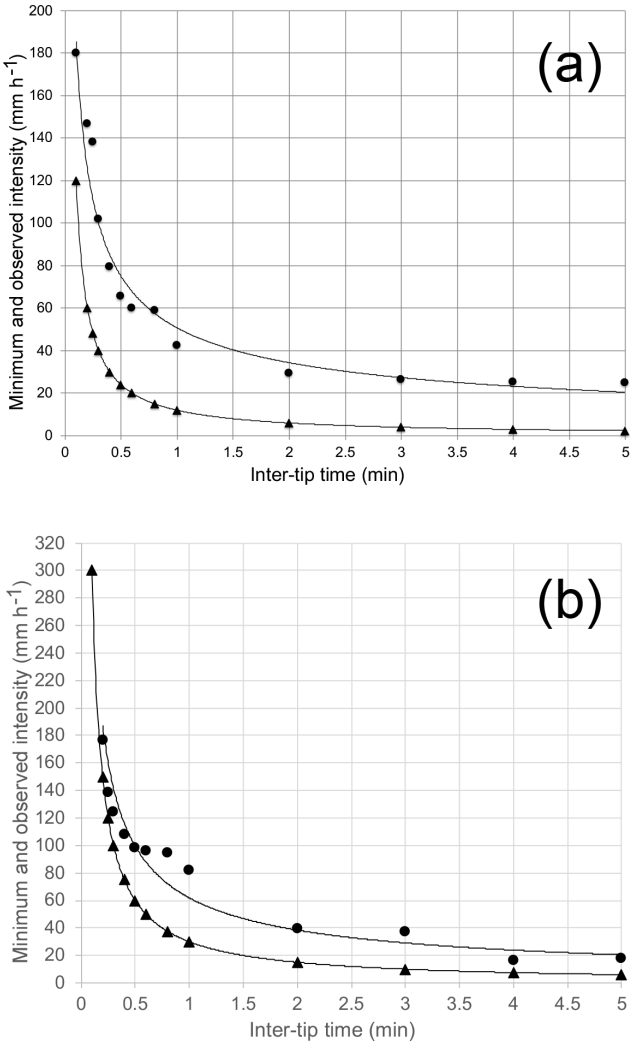

Figure 4. Expected intensity of intensity bursts of fixed ITTs having varying durations from 0.1 to 5 min (solid triangle symbols) and observed intensity of longest run of ITTs not exceeding each ITT (solid circle symbols). Locations: MM **(a)** and FG **(b)**. Fitted regression relations are shown by solid lines (for equations, see text). Note that in all cases, the observed intensities exceed those expected from fixed ITTs, indicating that the rainfall included some ITTs that were of shorter duration than the ITT indicated on the x axis.

shorter than indicated by the threshold ITT adopted to delineate them, since in all cases the calculated intensity of the recorded bursts exceeds the theoretical minimum intensity as shown in Fig. 4. This figure presents the observed intensity data for ITTs up to 5 min for both MM and FG, and it is evident that these exceed the nominal minimum intensity by an amount that increases for shorter ITTs. At MM the difference is about 20 mm h^{-1} for ITTs of more than $\sim$ 2 min but increases to about 90 mm h^{-1} for ITTs of $<$ 15 s, and a similar pattern is evident for FG.

The numbers of bucket tip events and the depth and duration of the longest run of successive ITTs not exceeding 5 min are shown in Fig. 5 for both FG and MM. The average intensity during the longest run is also shown for each ITT value.

The relationships among these run characteristics and the threshold ITT are generally well described by power functions. The mathematical relationship between runs of unvarying ITTs (in minutes) and the resulting rainfall intensity for MM can be described by the exact power function

$$\text{intensity (mm h}^{-1}) = 12\ \text{ITT}^{-1.0}. \quad (1)$$

For the relationship between the longest runs whose varying ITTs do not exceed nominated ITTs up to 5 min, the ob-

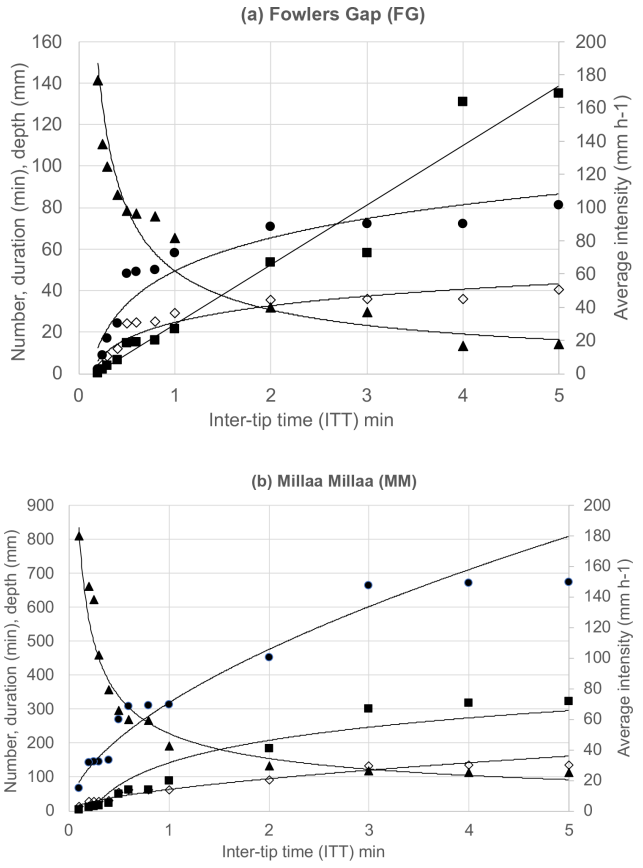

Figure 5. Data showing the characteristics of the longest run of ITTs not exceeding fixed thresholds of up to 5 min, for the rainfall records at Fowlers Gap (FG) **(a)** and for Millaa Millaa (MM) **(b)**. The average intensity of the longest run (solid triangle symbols) is plotted against the right-hand axis; the number of tip events in the longest run (solid circle symbols), the duration of the longest run (in minutes, solid square symbols), and the rainfall depth delivered by the longest run (open diamond symbols) are plotted against the left-hand axis.

served relationship for MM becomes

$$\text{intensity (mm h}^{-1}) = 50.73\ \text{ITT}^{-0.563}, \quad (2)$$

for which ITT is again expressed in minutes and $r^2 = 0.96$. For FG the corresponding relationship is

$$\text{intensity (mm h}^{-1}) = 61.88\ \text{ITT}^{-0.687}, \quad (3)$$

with $r^2 = 0.94$.

In terms of the longest bursts comprised of ITTs of less than 5 min, Fig. 6 shows that the intensity declines for longer runs, which are found for the larger values of ITT. The relationship for MM can be expressed as the power function

$$\text{intensity of longest run} = 423.6\ (\text{duration of longest run})^{-0.49}, \quad (4)$$

in which intensity is in mm h^{-1}, the duration of the longest run is expressed in minutes, and $r^2 = 0.98$. For FG, the corresponding relationship is

$$\text{intensity of longest run} = 199.4\ (\text{duration of longest run})^{-0.40}, \quad (5)$$

for which $r^2 = 0.80$.

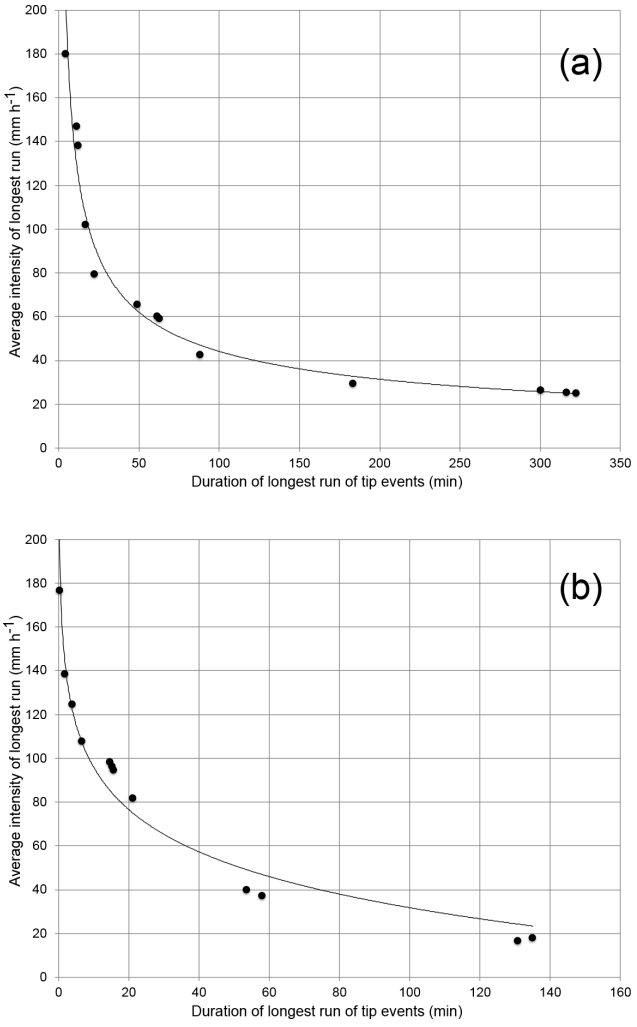

Figure 6. Relationships between the average intensity of the longest run of ITTs having durations from 0.1 to 5 min and the duration of the longest such run. Locations: **(a)** MM, **(b)** FG. The solid lines are fitted regression equations (see text for details). Note the rapid rise in intensity for bursts with durations less than about 20 min.

Are the nature and occurrence of intensity bursts different at the two field sites?

Table 2 shows that there are some notable similarities and differences between intensity bursts at the FG arid site and wet tropical MM. Maximum run durations for bursts exceeding the extreme intensity of 30 mm h^{-1} are comparable at the two sites – about 20 min. Burst durations for higher intensities become shorter, declining to 12–15 min for bursts of

$> 60\,\mathrm{mm\,h^{-1}}$. This is exceptionally intense rainfall. Despite the similarities of the bursts, their occurrence is very different. Table 2 shows the average time between the commencement of bursts. For example, bursts exceeding $60\,\mathrm{mm\,h^{-1}}$ at MM occur on average 39.1 h apart (1.6 d). In contrast, at FG events exceeding $60\,\mathrm{mm\,h^{-1}}$ are much less common, the average time between them being 36.9 d. The most intense bursts tabulated in Table 2, those exceeding $120\,\mathrm{mm\,h^{-1}}$, occur on average about every 4 d at MM but are much less frequent at FG, where they occur on average every 133 d (fewer than three occurrences per year). The other notable difference related to the climate of the two sites is the duration of intensity bursts. These are generally considerably longer at MM than at FG. For instance, bursts of $\sim 60\,\mathrm{mm\,h^{-1}}$ last for up to 60 min at MM but only for about 20 min at FG.

4 Discussion highlighting role of intensity bursts in land surface processes

The results just presented demonstrate the occurrence of bursts of rain many times more intense than hourly means – intensity bursts – and reaching intensities of 130–$180\,\mathrm{mm\,h^{-1}}$ over durations of approximately 5–15 min, and in some cases longer. Runs of ITTs of up to 5 min duration can last for hours and are striking features of the rainfall climatology but are too long to be considered "bursts" in the sense used here. Nevertheless, many are classified as showing extreme intensities (Tokay and Short, 1996). These data can be compared with the average rain day intensity of $0.48\,\mathrm{mm\,h^{-1}}$ or the average rain hour intensity of $1.43\,\mathrm{mm\,h^{-1}}$ noted earlier for MM. The intensity bursts are the kinds of short periods of intense rain that soil erosion researchers have sought to characterise by using fixed clock-period parameters such as I_{30} and I_{15}. Because it expresses the rainfall depth in the wettest 30 min period during a rainfall event, I_{30} is an equivalent intensity (the fixed intensity that would deliver the observed depth in 30 min) and does not necessarily capture the period of rainfall that has the highest actual intensity. Given that they have been used to successfully account for soil erosion (see later discussion), intensity bursts evidently deliver sufficiently intense rain to deepen surface ponding and so intensify soil splash dislodgment, establish overland flow paths by scouring the soil surface, and drive other surface processes explored below. The burst intensities are in some cases more than 2 orders of magnitude higher than even the mean rain hour intensity. The characteristics of intensity bursts in environments other than those studied here, such as those experiencing convective storms or frontal rain, appear to be largely unexplored. The intensity bursts have only been partially characterised here for illustrative purposes. A fuller analysis would consider their position within a rainfall event – early, middle, or late in the event, what relationship the bursts bear to the properties of the enclosing event, such as its total duration, depth, or mean intensity, and the frequency with which multiple bursts occur within an enclosing rainfall event. Some preliminary analyses of this kind were presented by Dunkerley (2013).

There are differences between indices such as I_{30}, which are derived from nominated clock periods, and measures based on runs of ITTs, which can begin and end at any instant and which can therefore have varying durations. The two measures yield results that are broadly comparable, though there are some significant differences. As an example, the observed I_{30} in the rainfall record at MM was $40.2\,\mathrm{mm\,h^{-1}}$, whereas Eq. (3) above suggests that an intensity burst of 30 min would have an intensity of $79.7\,\mathrm{mm\,h^{-1}}$. To the best of the writer's knowledge, no attempts have been made to relate measures of soil erosion to the duration and intensity of intensity bursts; rather, fixed clock periods such as I_{30} have always been used. It is possible to envisage that analyses of soil erosion could employ instead, for instance, the actual duration of intensity bursts of high intensity, highly erosive rainfall. Analyses might use the length of bursts with intensities of > 80 or $> 100\,\mathrm{mm\,h^{-1}}$, for instance. These burst characteristics are potentially more closely linked to processes occurring at the soil surface than the amount of rain in an arbitrary period such as 30 min. Thus, if an intensity burst at $80\,\mathrm{mm\,h^{-1}}$ and lasting 15 min occurred within an enclosing rainfall event that was mostly of $4\,\mathrm{mm\,h^{-1}}$ intensity, the I_{30} value, diluted by the inclusion of 15 min of low-intensity rain, would be about $42\,\mathrm{mm\,h^{-1}}$. Considering the hour enclosing the intensity burst, the apparent intensity would be just $23\,\mathrm{mm\,h^{-1}}$. This is $< 29\,\%$ of the true intensity of the potentially highly erosive intensity burst. These observations again underscore the potentially serious loss of information that may occur when rainfall data are aggregated to hourly, or even to 30 min, totals.

4.1 What evidence points to the significance of short-lived intensity bursts?

Multiple studies have shown that short-lived bursts are responsible for much of the runoff and erosion that takes place on agricultural, dryland, and other soils. Early studies of the importance of intensity peaks embedded within longer rainfalls include the work of Seginer et al. (1962) in Israel. In a study of runoff and soil loss using rainfall simulation, they adopted a 4.5 h design storm that included an intense central 30 min period preceded and followed by lower intensity rain. This central intense period caused most of the observed runoff and erosion. In a study of turbidity and sediment transport in a small Luxembourg catchment, Imeson (1977) logged stream turbidity at 1 min intervals and noted rapid fluctuations on this timescale. He related this to the sediment contributed by splash of soils from areas close to the channel, reporting that in a 2.2 h storm with an average intensity of 4–$4.5\,\mathrm{mm\,h^{-1}}$, the rainfall arrived as a series of very intense bursts separated by periods of lower intensity. Subsequent work has further explored effects of in-

tensity measured over timescales of a few minutes; only a few examples from a large body of literature are cited here. Mizugaki et al. (2010) showed that splash dislodgment of soil on Japanese forested hillslopes was strongly related to maximum rainfall intensity assessed in 10–30 min periods (I_{10}–I_{30}). Rainfall bursts extracted from data tallied over longer periods, such as hourly (I_{60}), proved to have less explanatory power. Likewise, Fraser et al. (2011) demonstrated the importance of I_{15} in erosion within the rangelands of northern Australia, and Wagenbrenner and Robichaud (2014) highlighted the importance of I_{10} in post-fire sediment movement in the western USA. At plot scale, Xia et al. (2013) showed that, for cropland in China, I_{10}, I_{20}, I_{30}, or I_{60} were significantly correlated with event losses of N and P and offered some hypotheses about why one or another index of intensity should become significant at a particular field site. Nunes et al. (2011) also stressed the explanatory power of I_{10} and I_{60} for erosion under various cover types in Portugal, as did Kiassari et al. (2012) for erosion plots in semi-arid Iran. At plot scale, the timing of intensity peaks within a rainfall event has been shown to greatly affect runoff ratios and depths, as well as peak runoff rate (Dunkerley, 2012). This effect is thought to arise partly as a result of the intensity peak occurring early, on dry soil, or later in the event when soils have been wetted up and infiltrability has declined as the wetting front progressed more deeply into the soil.

Erosion in post-fire landscapes can be especially intense. Even at larger hillslope scale within post-fire landscapes, Wagenbrenner and Robichaud (2014) showed strong correlations between the sediment yield delivered in runoff events and the I_{10} intensity of rainfall. However, as they emphasised, the landscape-scale effects may depend on the relative sizes of the burned area and the area covered by the intense rainfall burst. Small areas affected by intensity bursts may allow the runoff and sediment to be absorbed or attenuated when the runoff passes over unburned areas or areas not located within the area of intense rainfall. Again in the context of post-fire erosion, Hubbert et al. (2012) reported I_{10}, I_{30}, and I_{60} for field sites in southern California in the aftermath of chaparral fire and stressed the importance of intensity bursts, especially as expressed by I_{10}.

Short-period intensities have also been highlighted in unburned environments as well as in urban contexts. Taguas et al. (2010) analysed rainfall, runoff, and sediment yield data from a 6.1 ha Spanish catchment under olive cropping. They found strong correlations between I_{10} and runoff volume, runoff coefficient, the sediment concentration in runoff, and total sediment load. Correlations with I_{30} were smaller, a result attributed to the rapid hydrologic response of the catchment. For urban flash flooding arising from catchments draining the hinterland of Genoa (Liguria, Italy), Faccini et al. (2018) stressed the importance of rainfall intensities over periods of 1–3 h, while Papagiannaki et al. (2015) in Greece showed that urban flash flooding was probable for $I_{10} > 22.8\,\mathrm{mm\,h^{-1}}$ (or $I_{60} > 9.6\,\mathrm{mm\,h^{-1}}$). For Italy, Esposito et al. (2018) reported flash flood thresholds of $I_{10} > 54\,\mathrm{mm\,h^{-1}}$ or $I_{60} > 30\,\mathrm{mm\,h^{-1}}$. In catchments in SW Germany, Ruiz-Villanueva et al. (2012) showed that I_{30} offered less explanatory power than I_{60} for catchments $> 10\,\mathrm{km^2}$, owing to their longer response time (greater smoothing of the hydrologic response). For the tropical Lutzito rainforest catchment (3.3 ha) in Panama, Zimmermann et al. (2014) investigated the overland flow connectivity between hillslopes and the main channel. They stressed that short-term intensity measures such as I_5–I_{60} were important and also showed that the frequency with which the very short-lived intensity characterised by I_5 exceeds the soil saturated hydraulic conductivity (K_{sat}) has explanatory power, in the overland-flow-dominated runoff environment. It is possible that on hillslopes, overland flow paths become established during intensity bursts, and the establishment of connected runoff pathways may then facilitate runoff at lower intensities. This may be partly an effect of the clearing of mobile organic litter, which otherwise reduces flow speed and erodibility (Miyata et al., 2009; Ghahramani et al., 2011; Zhou et al., 2018), and perhaps some scour along flow pathways during the intensity bursts.

4.2 By what mechanisms do intensity bursts influence soil surface processes?

Here, a brief account is offered of some of the ways in which intensity bursts drive processes of soil erosion.

In terms of soil detachment by splash, an important mechanism linking intensity bursts to splash dislodgment of particles relates to the depth of ephemeral water ponding on the soil surface. Short bursts of intense rain, lasting perhaps minutes, are capable of exceeding the infiltrability of the soil surface, especially if they occur late in the rainfall event when the wetting front depth is greater and infiltrability is consequently lower (e.g. following the Horton exponential model – see Dunkerley, 2018). As a result, during an intensity burst, ephemeral ponding may appear in low-lying parts of the soil surface not previously ponded, and areas of existing shallow ponding may become deeper and cover larger areas. This is important because rates of soil detachment have been shown to increase rapidly as the water ponding depth increases, related to lateral jetting away from drop impact locations. This effect causes a rapid increase in splash detachment as ponding depths increase up to about three drop diameters, equivalent to perhaps 10 mm or so for typical raindrop diameters (Gao et al., 2003). As was shown by Timmons et al. (1971), drop impacts on ponding throw out splash droplets that are primarily made up of water from the ponding layer; surface tension limits the amount of water from an incident drop that becomes splash. Thus there are two consequences of the ponding effect on splash detachment: during an intensity burst, the area of ponding on the soil surface may increase, so enlarging the area over which active soil particle detachment can occur during the intensity burst. Second, existing areas of shallow ponding may be deepened and so enter the depth

range where splash is more intense. Simultaneously, some ponded areas may begin to show connected flow downslope, thus facilitating the movement of organic litter and soil particles. This suite of processes illustrates something of the level of process understanding required to resolve soil erosion processes at the level of detachment mechanisms. However, the experimental data cited earlier show that typically, the flux of splashed soil shows large increases during intensity bursts.

In addition to ponding, it is probable that other mechanisms at work at the soil surface are strongly activated during intensity bursts. The breakdown of soil aggregates prepares smaller, more readily transported particles, and this becomes more active with the higher kinetic energy expenditure at the soil surface associated with intensity bursts (Ewane and Lee, 2016). Additionally, air entrapment arises when drop bombardment of the soil surface forces air into the soil pore spaces. This reduces available infiltration pathways and by restricting infiltration rates, further encourages ephemeral surface ponding (Wang et al., 2014).

4.3 Short-term intensity bursts and climate change

Finally it is appropriate to consider the possible changes in the occurrence of short-lived intensity bursts in a future, warmer climate. Climate change is widely considered to be likely to result in more frequent extremes of rainfall, related in part to the increased moisture capacity of the atmosphere following the Clausius–Clapeyron relation, which suggests an increased moisture-holding capacity in association with warming of the atmosphere of $\sim 7\,\%\,^{\circ}C^{-1}$ (Fujibe, 2016). Wasko and Sharma (2015) reported that within sequences of rain hours, the most intense showed positive scaling with temperature, and the less intense, negative scaling. However, intensity bursts are an aspect of the intensity fluctuation that is characteristic of most rainfall events (Dunkerley, 2015) and it is not clear how the behaviour of these bursts – lasting only minutes or tens of minutes – might scale with temperature.

There have been multiple investigations of temporal trends in daily and hourly rainfall, based on time series of historical observations. Not all have found evidence of increasing rainfall extremes. Muschinski and Katz (2013) were able to find a significant rising trend for only one of 13 stations across the USA, primarily employing data from 1940 to 1999. Using data from 1942 to 2002, Soro et al. (2016) reported mostly decreasing trends in rainfall extremes for the Côte d'Ivoire. Barbero et al. (2017), using data from a large set of US data, found increasing annual maximum daily precipitation compatible with the expected CC scaling (they found $\sim 6.9\,\%\,^{\circ}C^{-1}$) but only a lesser scaling for hourly data. Fu et al. (2016) established a significant trend of increasing hourly rainfall over South China, using 31 years (1982–2012) of data from a large network of precipitation stations. They showed that an increasing frequency of rainfalls accounted for most of the observed effect, with only about 10 % attributable to changes in hourly intensity. Sun et al. (2017) analysed sub-daily rainfall (1–24 h) using 442 Chinese stations spanning 1960–2014 and showed complex regional variations in the trend to increasing or decreasing hourly extreme rainfalls.

A common approach to the analysis of extreme rainfall intensities is the use of downscaling from daily maxima to sub-daily values, though this is normally only extended to the prediction of hourly maxima. Sub-hourly rainfall data are generated in some micro-canonical cascade downscaling models (Jebari et al., 2012; Kianfar et al., 2016; Paschalis et al., 2014; Pohle et al., 2018) though with only moderate success in generating realistic intensities. Müller and Haberlandt (2018) for instance employed a micro-canonical cascade model and report overestimation of 5 min intensities of up to 63 %, though their "model B2" resulted in overestimates averaging only 11 %. As noted by Forestieri et al. (2018) downscaling can be undertaken by using correlations between daily and sub-daily maxima established from historical data, on the presumption that the correlations will remain invariant under climate change. Considering the probable effects of climate change for Sicily, via downscaling from a regional climate model (RCM), these authors derive estimated 1 h rainfall amounts for a 50-year return period of 42.05 mm (1972–2003 historical data), increasing by nearly 60 % (to 67.1 mm) for 2005–2050. For the USA, using quality-controlled empirical data, Barbero et al. (2017) found that the trend of rising annual daily maximum precipitation was approximately $7\,\%\,^{\circ}C^{-1}$, but there were only lower rates of change ($\sim 4\,\%\,^{\circ}C^{-1}$) for hourly extremes. In contrast, Chan et al. (2016) employed high-resolution convective-permitting RCM predictions of rainfall extremes down to 10 min timescales for the UK. They found that changes to modelled extremes for 10 min were very similar to those for 1 h duration. They note the need for observational data with which to better test model predictions. Given the importance of hourly sub-hourly precipitation for urban flooding, they argue for the acquisition of additional data on sub-hourly rainfall. Blenkinsop et al. (2018) have described the INTENSE project which is gathering such high-resolution rainfall observational data globally. Others (e.g. Prein et al., 2016) have argued that moist and dry environments exhibit different temperature scaling relationships, as a function of whether moisture is abundant or limiting. Evidently, much remains to be learned about sub-hourly rainfall and particularly how it may change globally and regionally under the predicted warmer climates of coming decades.

The intermittency of rainfall within rain days at the MM and FG field sites was noted earlier. This is another relatively under-studied aspect of rainfall climatology (Dunkerley, 2015). Schleiss (2018) demonstrated that failing to allow for the extent of intermittency of rainfall may lead to biased (under)estimates of the strength of the CC scaling and suggested a means to untangle the effects of temperature and intermittency on rainfall extremes. It has therefore to be remembered that extreme daily or hourly rainfall amounts are

not the same as extreme daily or hourly intensities, given that intermittency results in the daily or hourly rainfall amount being delivered in only a fraction of a day or hour.

4.4 The spatial variability of rainfall

This paper has addressed the temporal aspects of rainfall as it is recorded at a single point. The objective of the work was to highlight the occurrence of short-duration intensity bursts that can be identified when the rainfall data have an adequately fine temporal resolution. Intensity bursts were shown to be important to several land surface processes, including soil erosion. Accompanying the temporal variability of rainfall are spatial variations in duration, amount, and intensity, and these may occur over quite short distances (significant variability can be present over distances of hundreds of metres). Extreme convective events may result in very high rainfall amounts but over a limited areal extent (Einfalt et al., 1998). The rainfall may decline over 1–10 km scales and result in substantial underestimation of extreme rainfalls by the often more widely spaced gauges of precipitation observing networks (Schroeer et al., 2018). In many intense convective storms, the area affected is of the order of tens to hundreds of square kilometres; there are locations that appear to be "hotspots" for extreme precipitation events (Panziera et al., 2018). Moreover, higher temperatures may be associated with a decline in the extent of the most intense rainfall, as convection becomes increasingly localised (Peleg et al., 2018). Therefore, in seeking to understand the effect of rainfall variability on land surface processes, it would be desirable to acquire data on spatial intermittency as well as temporal intermittency. Further consideration of this aspect of rainfall variability is beyond the scope of this paper.

5 Conclusions

The brief snapshot of the role of intensity bursts across areas including soil erosion, the generation of overland flow, and urban flash flooding presented above shows that short-lived intensity bursts in rainfall have the potential to exert an important influence on diverse land surface processes. In terms of overland flow and soil erosion in particular, the intensity bursts are reasoned to act through several processes, not all of which are as yet completely understood, including effects on ponding depths at the soil surface, the breakdown of soil aggregates into smaller and more readily mobile particles, the establishment and linking of overland flow pathways, and probably the effects of air entrapment in reducing infiltration rates.

It would be valuable to have the capacity to predict trends in future soil erosion rates. It must be emphasised that this is a complex problem. Several examples of the role of intensity bursts cited above related to post-fire landscapes. Under future climates, many aspects of the factors influencing post-fire hillslope and channel erosion and their spatio-temporal extent may change. Not least among these is the foreshadowed increase in fire occurrence under future climates, which, through accelerated carbon loss, may feed back into further climate change. Rainfall intensity maxima thus form just one important component of a multi-faceted challenge to building informed land and environmental management for coming decades.

It is important to consider how intensity bursts might evolve in future climates, for which increased erosion risk has been foreshadowed. However, most contemporary observational rainfall data are too coarsely aggregated to permit the identification of intensity bursts. Therefore, we need more high-resolution data for two reasons. First, it will be important to understand more thoroughly the nature of intensity bursts in rainfall in different environments (arid, subhumid, wet tropical, etc.), a topic that is largely unexplored. This would then facilitate a more complete field-based and experimental analysis of how soil erosion rates relate to intensity bursts. In relation to soil erosion, including post-fire soil erosion, it is evident that the rainfall data need to have sufficient resolution for indices such as I_{10} to be determined. Second, a knowledge of intensity bursts can feed into and support attempts to develop improved downscaling methods from global and regional climate models, by drawing attention to aspects of sub-daily rainfall that are important in fields outside climate science. Contemporary observational data on short-term intensity bursts are desirable for parameterising and validating attempts to downscale predicted daily or hourly rainfalls to the important sub-hourly levels of aggregation, for which I_{30} or I_{10} may provide suitable indices. Rainfall data with high temporal resolution should ideally become more widely available to support research in soil erosion, flash flooding, and related areas. An ability to estimate the potential changes in short-term rainfall intensities such as I_{10} and I_{30}, and of intensity bursts generally, may be of great value in attempts to foreshadow likely rates of soil erosion under conditions of future invigorated rainfalls.

Data availability. The data analysed in this paper are not currently available online, as relevant permissions have not been received.

Competing interests. The author declares that there is no conflict of interest.

Acknowledgements. The author sincerely thanks Hannes Müller-Thomy and two anonymous reviewers for their insightful comments, which have helped to improve the argument and presentation of the work reported here.

Review statement. This paper was edited by Paola Passalacqua and reviewed by two anonymous referees.

References

Archer, D. R. and Fowler, H. J.: Characterising flash flood response to intense rainfall and impacts using historical information and gauged data in Britain, J. Flood Risk Manag., 11, 5121–5133, 2018.

Barbero, R., Fowler, H. J., Lenderink, G., and Blenkinsop, S.: Is the intensification of precipitation extremes with global warming better detected at hourly than daily resolutions?, Geophys. Res. Lett., 44, 974–983, https://doi.org/10.1002/2016GL071917, 2017.

Beranova, R., Kysely, J., and Hanel, M.: Characteristics of subdaily precipitation extremes in observed data and regional climate model simulations, Theor. Appl. Climatol., 132, 515–527, https://doi.org/10.1007/s00704-017-2102-0, 2018.

Blanco, H. and Lal, R.: Principles of Soil Conservation and Management, Springer, 616 pp. ISBN 978-1-4020-8708-0, 2008.

Blenkinsop, S., Fowler, H. J., Barbero, R., Chan, S. C., Guerreiro, S. B., Kendon, E., Lenderink, G., Lewis, E., Li, X.-F., Westra, S., Alexander, L., Allan, R. P., Berg, P., Dunn, R. J. H., Ekström, M., Evans, J. P., Holland, G., Jones, R., Kjellström, E., Klein-Tank, A., Lettenmaier, D., Mishra, V., Prein, A. F., Sheffield, J., and Tye, M. R.: The INTENSE project: using observations and models to understand the past, present and future of sub-daily rainfall extremes, Adv. Sci. Res., 15, 117–126, https://doi.org/10.5194/asr-15-117-2018, 2018.

Bowman, D. M. J. S., Murphy, B. P., Boer, M. M., Bradstock, R. A., Cary, G. J., Cochrane, M. A., Fensham, R. J., Krawchuk, M. A., Price, O. F., and Williams, R. J. Forest Area management, climate change, and the risk of catastrophic carbon losses, Front. Ecol. Environ., 11, 66–68, https://doi.org/10.1890/13.WB.005, 2013.

Chan, S. C., Kendon, E. J., Roberts, N. M., Fowler, H. J., and Blenkinsop, S.: The characteristics of summer sub-hourly rainfall over the southern UK in a high-resolution convective permitting model, Environ. Res. Lett., 11, 094024, https://doi.org/10.1088/1748-9326/11/9/094024, 2016.

Cortés-Hernández, V. E., Zheng, F., Evans, J., Lambert, M., Sharma, A., and Westra, S.: Evaluating regional climate models for simulating sub-daily rainfall extremes, Clim. Dynam., 47, 1613–1628, https://doi.org/10.1007/s00382-015-2923-4, 2016.

Costa, A. C. and Soares, A.: Trends in extreme precipitation indices derived from a daily rainfall database for the South of Portugal, Int. J. Climatol., 29, 1956–1975, https://doi.org/10.1002/joc.1834, 2008.

de Waal, J. H., Chapman, A., and Kemp, J.: Extreme 1-day rainfall distributions: Analysing change in the Western Cape, S. Afr. J. Sci., 113, 8 pp., https://doi.org/10.17159/sajs.2017/20160301, 2017.

Donat, M. G., Alexander, L. V., Yang, H., Durre, I., Vose, R., Dunn, R. J. H., Willett, K. M., Aguilar, E., Brunet, M., Caesar, J., Hewitson, B., Jack, C., Klein Tank, A. M. G., Kruger, A. C., Marengo, J., Peterson, T. C., Renom, M., Oria Rojas, C., Rusticucci, M., Salinger, J., Elrayah, A. S., Sekele, S. S., Srivastava, A. K. Trewin, B., Villarroel, C., Vincent, L. A., Zhai, P., Zhang, X., Kitching, S.: Updated analyses of temperature and precipitation extreme indices since the beginning of the twentieth century: The HadEX2 dataset, J. Geophys. Res.-Atmos., 118, 2098–2118, https://doi.org/10.1002/jgrd.50150, 2013.

Dong, G., Weng, B., Qin, T., Yan, D., Wang, H., Gong, B., Bi, W., and Xing, Z.: The Impact of the Construction of Sponge Cities on the Surface Runoff in Watersheds, China, Adv. Meteorol., 2018, 6241892, https://doi.org/10.1155/2018/6241892, 2018.

Dunkerley, D. L: Identifying individual rain events from pluviograph records: a review with analysis of data from an Australian dryland site, Hydrol. Process., 22, 5024–5036, https://doi.org/10.1002/hyp.7122, 2008.

Dunkerley, D. L.: How do the rain rates of sub-event intervals such as the maximum 5- and 15-min rates (I_5 or I_{30}) relate to the properties of the enclosing rainfall event?, Hydrol. Process., 24, 2425–2439, https://doi.org/10.1002/hyp.7650, 2010.

Dunkerley, D. L.: Effects of rainfall intensity fluctuations on infiltration and runoff: rainfall simulation on dryland soils, Fowlers Gap, Australia, Hydrol. Process., 26, 2211–2224, https://doi.org/10.1002/hyp.8317, 2012.

Dunkerley, D. L.: Sub-daily rainfall events in an arid environment with marked climate variability: Variation among wet and dry years at Fowlers Gap, New South Wales, Australia, J. Arid Environ., 96, 23–30, https://doi.org/10.1016/j.jaridenv.2013.04.002, 2013.

Dunkerley, D. L.: Intra-event intermittency of rainfall: an analysis of the metrics of rain and no-rain periods, Hydrol. Process., 29, 3294–3305, https://doi.org/10.1002/hyp.10454, 2015.

Dunkerley, D. L.: How is overland flow produced under intermittent rain? An analysis using plot-scale rainfall simulation on dryland soils, J. Hydrol., 556, 119–130, https://doi.org/10.1016/j.jhydrol.2017.11.003, 2018.

Einfalt, T., Johann, G., and Pfister, A.: On the spatial validity of heavy point rainfall measurements, Water Sci. Technol., 37, 21–28, 1998.

Esposito, G., Matano, F., and Scepi, G.: Analysis of increasing flash flood frequency in the densely urbanized coastline of the Campi Flegrei volcanic area, Italy, Front. Earth Sci., 6, 63, https://doi.org/10.3389/feart.2018.00063, 2018.

Ewane, E. B. and Lee, H. H.: Effects of vegetation cover on sediment particle size distribution and transport processes in natural rainfall conditions on post-fire hillslope plots in South Korea, Soil Res., 54, 937–948, https://doi.org/10.1071/SR16117, 2016.

Faccini, F., Luino, F., Paliaga, G., Sacchini, A., Turconi, L., and de Jong, C.: Role of rainfall intensity and urban sprawl in the 2014 flash flood in Genoa City, Bisagno catchment (Liguria, Italy), Appl. Geogr., 98, 224–241, https://doi.org/10.1016/j.apgeog.2018.07.022, 2018.

Forestieri, A., Arnone, E., Blenkinsop, S., Candela, A., Fowler, H., and Noto, L. V.: The impact of climate change on extreme precipitation in Sicily, Italy, Hydrol. Process., 32, 332–348, https://doi.org/10.1002/hyp.11421, 2018.

Formayer, H. and Fritz, A.: Temperature dependency of hourly precipitation intensities – surface versus cloud layer temperature, Int. J. Climatol., 37, 1–10, https://doi.org/10.1002/joc.4678, 2017.

Fraser, G. W., Carter, J. O., McKeon, G. M., and Day, K. A.: A new empirical model of sub-daily rainfall intensity and its application in a rangeland biophysical model, Rangeland J., 33, 37–48, https://doi.org/10.1071/RJ10037, 2011.

Fu, Y., Li, G., and Zheng, T.: Impact of raindrop characteristics on the selective detachment and transport of aggregate fragments in

the Loess Plateau of China, Soil Sci. Soc. Am. J., 80, 1071–1077, https://doi.org/10.2136/sssaj2016.03.0084, 2016.

Fujibe, F.: Annual Variation of Extreme Precipitation Intensity in Japan: Assessment of the Validity of Clausius-Clapeyron Scaling in Seasonal Change, SOLA, 12, 106–110, https://doi.org/10.2151/sola.2016-024, 2016.

Gao, B., Walter, M. T., Steenhuis, T. S., Parlange, J.-Y., Nakano, K., Rose, C. W., and Hogarth, W. L.: Investigating ponding depth and soil detachability for a mechanistic erosion model using a simple experiment, J. Hydrol., 277, 116–124, 2003.

Gao, Y., Xiao, L., Chen, D., Xu, J., and Zhang, H.: Comparison between past and future extreme precipitations simulated by global and regional climate models over the Tibetan Plateau, Int. J. Climatol., 38, 1285–1297, https://doi.org/10.1002/joc.5243, 2018.

Garbrecht, J. D., Nearing, M. A., Steiner, J. L., Zhang, X. J., and Nichols, M. H.: Can conservation trump impacts of climate change on soil erosion? An assessment from winter wheat cropland in the Southern Great Plains of the United States, Weather Clim. Extremes, 10, 32–39, https://doi.org/10.1016/j.wace.2015.06.002, 2015.

Ghahramani, A., Ishikawa, Y., and Gomi, T.: Slope length effect on sediment and organic litter transport on a steep forested hillslope: upscaling from plot to hillslope scale, Hydrological Research Letters, 5, 16–20, https://doi.org/10.3178/HRL.5.16, 2011.

Giang, P. Q., Giang, L. T., and Toshiki, K.: Spatial and Temporal Responses of Soil Erosion to Climate Change Impacts in a Transnational Watershed in Southeast Asia, Climate, 5, 22, https://doi.org/10.3390/cli5010022, 2017.

Guerreiro S. B., Fowlers, H. J., Barbero, R., Westra, S., Lenderink, G., Blenkinsop, S., Lewis, E., and Li, X.-F.: Detection of continental-scale intensification of hourly rainfall extremes, Nat. Clim. Change, 8, 803–807, https://doi.org/10.1038/s41558-018-0245-3, 2018.

Harvey, B. J.: Human-caused climate change is now a key driver of forest fire activity in the western United States, P. Natl. Acad. Sci. USA, 113, 11649–11650, https://doi.org/10.1073/pnas.1612926113, 2016.

Hatfield, J. L., Cruse, R. M., and Tomer, M. D.: Convergence of agricultural intensification and climate change in the Midwestern United States: implications for soil and water conservation, Mar. Freshwater Res., 64, 423–435, https://doi.org/10.1071/MF12164, 2013.

Hatzaki, M., Flocas, H. A., Oikonomou, C., and Giannakopoulos, C.: Future changes in the relationship of precipitation intensity in Eastern Mediterranean with large scale circulation, Adv. Geosci., 23, 31–36, https://doi.org/10.5194/adgeo-23-31-2010, 2010.

Hubbert, K. R., Wohlgemuth, P. M., and Beyers, J. L.: Effects of hydromulch on post-fire erosion and plant recovery in chaparral shrublands of southern California, Int. J. Wildland Fire, 21, 155–167, https://doi.org/10.1071/WF10050, 2012.

Imeson, A. C.: Splash erosion, animal activity and sediment supply in a small forested Luxembourg catchment, Earth Surf. Proc. Land., 2, 153–160, 1977.

Jebari, S., Berndtsson, R., Olsson J., and Bahri, A.: Soil erosion estimation based on rainfall disaggregation, J. Hydrol., 436–437, 102–110, https://doi.org/10.1016/j.jhydrol.2012.03.001, 2012.

Karmakar, R., Das, I., Dutta, D., and Rakshit, A.: Potential Effects of Climate Change on Soil Properties: A review, Science International, 4, 51–73, https://doi.org/10.17311/sciintl.2016.51.73, 2016.

Keggenhoff, I., Elizbarashvili, M., Amiri-Farahani, A., and King, L.: Trends in daily temperature and precipitation extremes over Georgia, 1971–2010, Weather and Climate Extremes, 4, 75–85, https://doi.org/10.1016/j.wace.2014.05.001, 2014.

Kianfar, B., Fatichi, S., Paschalis, A., Maurer, M., and Molnar, P.: Climate change and uncertainty in high-resolution rainfall extremes, Hydrol. Earth Syst. Sci. Discuss., https://doi.org/10.5194/hess-2016-536, in review, 2016.

Kiassari, E. M., Nikkami, D., Mahdian, M. H., and Pazira, E.: Investigating rainfall erosivity indices in arid and semi-arid climates of Iran, Turk. J. Agric. For., 36, 365–378, https://doi.org/10.3906/tar-1103-9, 2012.

Klik, A. and Eitzinger, J.: Impact of climate change on soil erosion and the efficiency of soil conservation practices in Austria, J. Agr. Sci., 148, 529–541, https://doi.org/10.1017/S0021859610000158, 2010.

Li, Z., and Fang, H.: Impacts of climate change on water erosion: A review, Earth-Sci. Rev., 163, 94–117, https://doi.org/10.1016/j.earscirev.2016.10.004, 2016.

Li, H., Ding, L., Ren, M., Li, C., and Wang, H.: Sponge City Construction in China: A Survey of the Challenges and Opportunities, Water, 9, 594, https://doi.org/10.3390/w9090594, 2017.

Li, J., Zhang, B., Mu, C., and Chen, L.: Simulation of the hydrological and environmental effects of a sponge city based on MIKE FLOOD, Environ. Earth Sci., 77, 32, https://doi.org/10.1007/s12665-018-7236-6, 2018.

Luo, L. and Wang, Z.: Changes in hourly precipitation may explain the sharp reduction of discharge in the middle reach of the Yellow River after 2000, Front. Environ. Sci. En., 7, 756–768, https://doi.org/10.1007/s11783-013-0563-7, 2013.

Lupikasza, E. B.: Seasonal patterns and consistency of extreme precipitation trends in Europe, December 1950 to February 2008, Clim. Res., 72, 217–237, https://doi.org/10.3354/cr01467, 2017.

Miyata, S., Kosugi, K., Gomi, T., and Mizuyama, T.: Effects of forest floor coverage on overland flow and soil erosion on hillslopes in Japanese cypress plantation forests, Water Resour. Res., 45, W06402, https://doi.org/10.1029/2008WR007270, 2009.

Mizugaki, S., Nanko, K., and Onda, Y.: The effect of slope angle on splash detachment in an unmanaged Japanese cypress plantation forest, Hydrol. Process., 24, 576–587https://doi.org/10.1002/hyp.7552, 2010.

Mondal, A., Khare, D., Kundu, S., Meena, P.K., Mishra, P.K., and Shukla, R.: Impact of Climate Change on Future Soil Erosion in Different Slope, Land Use, and Soil-Type Conditions in a Part of the Narmada River Basin, India, J. Hydrol. Eng., 20, C5014003, https://doi.org/10.1061/(ASCE)HE.1943-5584.0001065, 2015.

Monjo, R.: Measure of rainfall time structure using the dimensionless n-index, Clim. Res., 67, 71–86, https://doi.org/10.3354/cr01359, 2016.

Mullan, D., Favis-Mortlock, D., and Fealy, R.: Addressing key limitations associated with modelling soil erosion under the impacts of future climate change, Agr. Forest Meteorol., 156, 18–30, https://doi.org/10.1016/j.agrformet.2011.12.004, 2012.

Müller, H. and Haberlandt, U.: Temporal rainfall disaggregation using a multiplicative cascade model for spatial application in urban hydrology, J. Hydrol., 556, 847–864, https://doi.org/10.1016/j.jhydrol.2016.01.031, 2018.

Muschinski, T. and Katz, J. I.: Trends in hourly rainfall statistics in the United States under a warming climate, Nat. Clim. Change, 3, 577–580, https://doi.org/10.1038/nclimate1828, 2013.

Nandargi, S. and Mulye, S. S.: Relationships between Rainy Days, Mean Daily Intensity, and Seasonal Rainfall over the Koyna Catchment during 1961–2005, Sci. World J., 2012, 894313, https://doi.org/10.1100/2012/894313, 2012.

Nearing, M. A., Pruski, F. F., and O'Neal, M. R.: Expected climate change impacts on soil erosion: a review, J. Soil Water Conserv., 59, 43–50, 2004.

Nunes, A. N., de Almeida, A. C., and Coelho, C. O. A.: Impacts of land use and cover type on runoff and soil erosion in a marginal area of Portugal, Appl. Geogr., 31, 687–699, https://doi.org/10.1016/j.apgeog.2010.12.006, 2011.

O'Gorman, P. A. and Schneider, T.: The physical basis for increases in precipitation extremes in simulations of 21st-century climate change, P. Natl. Acad. Sci. USA, 106, 14773–14777, https://doi.org/10.1073/pnas.0907610106, 2009.

Panagos, P., Borrelli, P., Poesen, J., Ballabio, C., Lugato, E., Meusberger, K., Montanarella, L., and Alewell, C.: The new assessment of soil loss by water erosion in Europe, Environ. Sci. Policy, 54, 438–447, https://doi.org/10.1016/j.envsci.2015.08.012, 2015.

Panziera, L., Gabella, M., Germann, U., and Martius, O.: A 12-year radar-based climatology of daily and sub-daily extreme precipitation over the Swiss Alps, Int. J. Climatol., 38, 3749–3769, https://doi.org/10.1002/joc.5528, 2018.

Papagiannaki, K., Lagouvardos, K., Kotroni, V., and Bezes, A.: Flash flood occurrence and relation to the rainfall hazard in a highly urbanized area, Nat. Hazards Earth Syst. Sci., 15, 1859–1871, https://doi.org/10.5194/nhess-15-1859-2015, 2015.

Paschalis, A., Molnar, P., Fatichi, S., and Burlando, P.: On temporal stochastic modeling of precipitation, nesting models across scales, Adv. Water Resour., 63, 152–186, https://doi.org/10.1016/j.advwatres.2013.11.006, 2014.

Peleg, N., Marra, F., Fatichi, F., Molnar, P., Morin, E., Sharma, A., and Burlando, P.: Intensification of Convective Rain Cells at Warmer Temperatures Observed from High-Resolution Weather Radar Data, J. Hydrometeorol., 19, 715–726, https://doi.org/10.1175/JHM-D-17-0158.1, 2018.

Pendergrass, A. G. and Deser, C.: Climatological characteristics of typical daily precipitation, J. Climate, 30, 5985–6003, https://doi.org/10.1175/JCLI-D-16-0684.1, 2017.

Peters, O. and Christensen, K.: Rain: relaxations in the sky, Phys. Rev. E., 66, 036120, https://doi.org/10.1103/PhysRevE.66.036120, 2002.

Peralta-Hernández, A. R., Balling, R. C., and Barba-Martínez, L. R.: Comparative analysis of indices of extreme rainfall events: Variations and trends from southern México, Atmósfera, 22, 219–228, 2009.

Pohle, I., Niebisch, M., Müller, H., Schümberg, S., Zha, T., Maurer, T., and Hinz, C.: Coupling Poisson rectangular pulse and multiplicative microcanonical random cascade models to generate sub-daily precipitation timeseries, J. Hydrol., 562, 50–70, https://doi.org/10.1016/j.jhydrol.2018.04.063, 2018.

Polemio, M. and Lonigro, T.: Trends in climate, short-duration rainfall, and damaging hydrogeological events (Apulia, Southern Italy), Nat. Hazards, 75, 515–540, https://doi.org/10.1007/s11069-014-1333-y, 2015.

Prein, A. F., Rasmussen, R. M., Ikeda, K., Liu, C., Clark, M. P., and Holland, G. J.: The future intensification of hourly precipitation extremes, Nat. Clim. Change, 7, 48–53, https://doi.org/10.1038/NCLIMATE3168, 2016.

Rhodes, C. J.: Soil erosion, climate change and global food security: challenges and strategies, Sci. Progress., 97, 97–153, https://doi.org/10.3184/003685014X13994567941465, 2014.

Ruiz-Villanueva, V., Borga, M., Zoccatelli, D., Marchi, L., Gaume, E., and Ehret, U.: Extreme flood response to short-duration convective rainfall in South-West Germany, Hydrol. Earth Syst. Sci., 16, 1543–1559, https://doi.org/10.5194/hess-16-1543-2012, 2012.

Schär, C., Ban, N., Fischer, E.M., Rajczak, J., Schmidli, J., Frei, C., Giorgi, F., Karl, T. R., Kendon, E. J., Klein Tank, A. M. G., O'Gorman, P. A., Sillmann, J., Zhang, X., and Zwiers, F. W.: Percentile indices for assessing changes in heavy precipitation events, Clim. Change, 137, 201–216, https://doi.org/10.1007/s10584-016-1669-2, 2016.

Schleiss, M.: How intermittency affects the rate at which rainfall extremes respond to changes in temperature, Earth Syst. Dynam., 9, 955–968, https://doi.org/10.5194/esd-9-955-2018, 2018.

Schroeer, K., Kirchengast, G., and O, S.: Strong Dependence of Extreme Convective Precipitation Intensities on Gauge Network Density, Geophys. Res. Lett., 45, 8253–8263, https://doi.org/10.1029/2018GL077994, 2018.

Seginer, I., Morin, J., and Shachori, A.: Runoff and erosion studies in a mountainous terra-rossa region, International Association of Scientific Hydrology, Bulletin, 7, 79–92, https://doi.org/10.1080/02626666209493284, 1962.

Segura, C., Sun, G., McNulty, S., and Zhang, Y.: Potential impacts of climate change on soil erosion vulnerability across the conterminous United States, J. Soil Water Conserv., 69, 171–181, https://doi.org/10.2489/jswc.69.2.171, 2014.

Sharratt, B. S., Tatarko, J., Abatzoglou, J. T., Fox, F. A., and Huggins, D.: Implications of climate change on wind erosion of agricultural lands in the Columbia plateau, Weather and Climate Extremes, 10, 20–31, https://doi.org/10.1016/j.wace.2015.06.001, 2015.

Soro, G. E., Noufé, D., Bi, T. A. G., and Shorohou, B.: Trend Analysis for Extreme Rainfall at Sub-Daily and Daily Timescales in Cô te d'Ivoire, Climate, 4, 37, https://doi.org/10.3390/cli4030037, 2016.

Sun, H., Wang, G., Li, X., Chen, J., Su, B., and Jiang, T.: Regional Frequency Analysis of Observed Sub-Daily Rainfall Maxima over Eastern China, Adv. Atmos. Sci., 34, 209–225, https://doi.org/10.1007/s00376-016-6086-y, 2017.

Taguas, E. V., Peña, A., Ayuso, J. L., Pérez, R., Yuan, Y., and Giráldez, J. V.: Rainfall variability and hydrological and erosive response of an olive tree microcatchment under no-tillage with a spontaneous grass cover in Spain, Earth Surf. Proc. Land., 35, 750–760, https://doi.org/10.1002/esp.1893, 2010.

Timmons, D. R., Mutchler, C. K., and Sherstad, E. M.: Use of Fluoresceine to Measure the Composition of Waterdrop splash, Water Resour. Res., 7, 1020–1023, 1971.

Tokay, A. and Short, D. A.: Evidence from tropical raindrop spectra of the origin of rain from stratiform versus convective clouds, J. Appl. Meteorol., 35, 355–371, 1996.

van Bellen, S., Garneau, M., and Bergeron, Y.: Impact of climate change on forest fire severity and consequences for carbon stocks

in boreal forest stands of Quebec, Canada: a synthesis, Fire Ecol., 6, 16–44, https://doi.org/10.4996/fireecology.0603016, 2010.

Wagenbrenner, J. W. and Robichaud, P. R.: Post-fire bedload sediment delivery across spatial scales in the interior western United States, Earth Surf. Proc. Land., 39, 865–876, https://doi.org/10.1002/esp.3488, 2014.

Wang, J. C., Gong, X. N., and Ma, S. G.: Modification of Green-Ampt Infiltration Model Considering Entrapped Air Pressure, Electronic Journal of Geotechnical Engineering (EJGE), 19, 1801–1811, 2014.

Wasko, C. and Sharma, A.: Steeper temporal distribution of rain intensity at higher temperatures within Australian storms, Nat. Geosci., 8, 527–529, https://doi.org/10.1038/ngeo2456, 2015.

Xia, L., Hoermann, G., Ma, L., and Yang, L.: Reducing nitrogen and phosphorus losses from arable slope land with contour hedgerows and perennial alfalfa mulching in Three Gorges Area, China, Catena, 110, 86–94, https://doi.org/10.1016/j.catena.2013.05.009, 2013.

Yilmaz, A. G. and Perera, B. J. C.: Spatiotemporal Trend Analysis of Extreme Rainfall Events in Victoria, Australia, Water Resour. Manag., 29, 4665–4480, https://doi.org/10.1007/s11269-015-1070-3, 2015.

Yu, L., Zhong, S., Heilman, W. E., and Bian, X.: A comparison of the effects of El Niño and El Niño Modoki on subdaily extreme precipitation occurrences across the contiguous United States, J. Geophys. Res.-Atmos., 122, 7401–7415, https://doi.org/10.1002/2017JD026683, 2017.

Zhang, X., Alexander, L., Hegerl, G. C., Jones, P., Tank, A. K., Peterson, T. C., Trewin, B., and Zwiers, F. W.: Indices for monitoring changes in extremes based on daily temperature and precipitation data, WIREs Clim. Change, 2, 851–870, https://doi.org/10.1002/wcc.147, 2011.

Zhou, Q., Zhou, X., Luo, Y., and Cai, M.: The Effects of Litter Layer and Topsoil on Surface Runoff during Simulated Rainfall in Guizhou Province, China: A Plot Scale Case Study, Water, 10, 915, https://doi.org/10.3390/w10070915, 2018.

Zimmermann, B., Zimmermann, A., Turner, B. L., Francke, T., and Elsenbeer, H.: Connectivity of overland flow by drainage network expansion in a rain forest catchment, Water Resour. Res., 50, 1457–1473, https://doi.org/10.1002/2012WR012660, 2014.